

# Ultra-wideband Flexible Implantable Antenna for Wireless Capsule Endoscopy System with Performance Improvement

Yang Feng, Pan Chen, Shaopeng Pan, and Gaosheng Li\*

College of Electrical and Information Engineering, Hunan University, Changsha 410082, China

\*gaosheng7070@vip.163.com

**Abstract** — The implantable antenna is an important part of the wireless capsule endoscopy (WCE) system to achieve wireless communication. This paper designed an ultra-wideband flexible implantable antenna for wireless capsule endoscopy system. With a very wide bandwidth, the antenna can completely cover the industrial, scientific, and medical frequency bands (ISM, 2.4-2.48 GHz) and Wireless Medical Telemetry Service (WMTS, 1.395-1.4 GHz). The expanded size of the proposed antenna is 18mm× 10mm× 0.1mm. The conformal technology of the antenna has further reduced the space of the system and achieved miniaturization. The capsule antenna in this paper is a compact planar monopole antenna fed by a coplanar waveguide, and it uses a flexible material as a dielectric substrate to achieve the conformal shape of the antenna. U-shaped ground branch (UGB) and a loaded split ring resonator (SRR) structure were used to further improve the antenna performance. Simulation and measurement results were basically the same. On the premise of radiation safety and miniaturization of the antenna, the ultra-wideband operation of the antenna was realized. This antenna design provided reference value for the design and application of the capsule antenna.

**Index Terms** — Conformal, implantable antenna, ultra-wideband, wireless capsule endoscopy system.

## I. INTRODUCTION

Miniature implantable medical devices are commonly used for disease treatment and physiological testing, providing a higher quality of protection for people's health. In the field of electronic medicine, the wireless capsule endoscopy (WCE) system is a non-invasive gastrointestinal detection system that acquires image data of the digestive tract and wirelessly transmits it to determine the physiological condition of the human body [1]. The antenna is a bridge to realize the communication between the wireless capsule endoscopic system and the outside world by performing information transmission and wireless energy transmission and other task. Moreover, more requirements are put forward for the performance of the implanted antenna [2] in that the biological tissue structure of the human body features

high dielectric constant and high loss. In addition, the need to miniaturize the wireless capsule endoscopy system, required us to reduce the overall volume of the antenna to save system space. To fully utilize the space, the antenna formed a conformal structure on the inner wall of the capsule [3-4]. The structure can save more space in the system and further realize the miniaturization of the system. It can also make full use of the surface for radiation and increase the working bandwidth of the antenna [5]. The flexible capsule implantable antenna is of great practical value in the application research of telemetry biomedicine.

In recent years, many scientific research teams have carried out exploration and research on the performance and size of the capsule antennas. Different types of capsule antennas used in different working environments. A capsule microstrip antenna working in ISM frequency band was designed [6] to cater to the requirements of the telemetry capsule in human digestive tract system. In addition, [7] designed a broadband capsule antenna for the Medical Device Radiocommunications Service (MedRadio, 401-406 MHz) frequency band. The antenna loads a metal branch in the center of the zigzag dipole, and adjusts the length of the metal branch to excite another resonance point, which increases the working bandwidth. An implantable capsule conformal antenna was designed to operate in the MediRadio frequency band for WCE [8], in which a zigzag line was adopted to increase the bandwidth, and the peak gain was -31.5 dBi. [9] also proposed an ultra-wideband capsule antenna, which covered the MICS and ISM frequency bands and achieved omnidirectional radiation, but the maximum gain was only -31.5 dBi. [10] proposed a conformal patch antenna design with CSRR loading. However, this was a single narrowband (2.45 GHz) design. A wideband flexible loop antenna loaded with a split ring resonator (SRR) was designed to achieve ultra-wideband operation. The return loss of the antenna was improved by the SRR, and the absorbed power of the human body was reduced [11]. In [12], this paper designed a capsule antenna that works at ISM with a thickness of only 0.1 mm. The size was reduced by geometric fractal, and the antenna gain was -30.6 dBi.

Compared with the general fixed implantable antenna, the antenna of the wireless capsule endoscopy (WCE) system is more flexible and its working environment is more complicated. Since the dielectric properties of human tissues are very complex and changeable, the resonance frequency is prone to shift, so a wide bandwidth is required. The ultra-wideband performance of the capsule antenna helps to resist the frequency shift effect, especially when the capsule is close to different tissues of the intestine and stomach. Further investigation has found that the capsule conformal antenna mainly needs to be improved in two aspects. On the one hand, due to the small size of the capsule itself, miniaturization is the eternal topic of capsule antenna design. While ensuring the performance of the antenna, new methods are still needed to achieve further miniaturization of the antenna size; on the other hand, the antenna design must also consider the ratio absorption rate (SAR), gain and power at the same time. It is still a promising subject to design a compact flexible antenna that can cover multiple operating frequency bands and has good radiation characteristics. In this paper, based on a coplanar waveguide fed planar monopole antenna, the antenna was designed in view of the compact structure of the wireless capsule endoscopy system and the diverse working environment. The antenna was designed using U-shaped ground branch (UGB), radiative patch slotting and loaded split ring resonator (SRR) technology. The antenna realized the ultra-wideband operation of the antenna, covering the two frequency bands of WMTS and ISM for the operation of the implantable antenna, and the frequency range of the antenna was 1.15 - 4.18 GHz. The volume of the antenna was 18 mm<sup>3</sup>. Considering the miniaturization and performance, this design can save more space in the capsule endoscopic system while realizing the wide bandwidth and miniaturization of the antenna. This paper is organized as follows: The method is introduced in the second part. The third section introduces the design and optimization of the antenna. The fourth section introduces the antenna design results and discussion. Section five summarizes the conclusions.

## II. METHODOLOGY

### A. Antenna structure design

The planar monopole antenna has the advantages of thin profile, small size, low manufacturing cost, and wide frequency band. Combined with the space structure in the capsule system, a planar monopole antenna is a good choice. To reach the required working frequency band of the antenna, we conducted a preliminary design based on the principle, the formula is as follows:

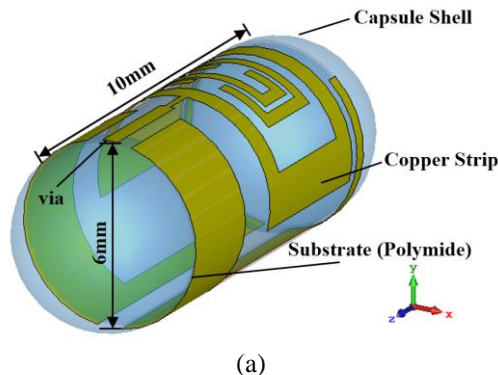
$$f = \frac{c}{4l\sqrt{\epsilon_r}}, \quad (1)$$

where  $l$  is the effective length,  $c$  is the speed of light in free space, and  $f$  is the frequency.

We can know that the effective current path is inversely proportional to the frequency when the dielectric constant is constant. Through (1), a better approximation can be obtained, and the antenna model can be preliminarily designed. In the actual design process, the design can be optimized based on the initial size.

The design adopted the conformal technology of the antenna and the electronic capsule endoscope system, which reduced the space occupation of the system. In this design, the same material as [13] and ( $\epsilon_r = 3.5$ ,  $\tan\delta = 0.0027$ ) was used as the dielectric substrate of the antenna. The thickness of the dielectric substrate of the antenna was 0.1 mm. The unfolded size of the antenna was only 18 mm×10 mm×0.1 mm. The radius of the antenna after conformal in the capsule was 3 mm. The capsule antenna structure is shown in Fig. 1.

The flexible material features strong environmental adaptability, and the dielectric substrate of the antenna can be more suitable for the structure of the system. Conformal processing of the antenna will not affect its performance [2]. It adopts a single-layer metal structure, which is mainly composed of a radiating surface and a dielectric substrate. The antenna feed adopts coplanar waveguide feed. The coplanar waveguide feeding structure has low cost and low parasitic parameters. The radiating unit and the feeding unit in this way are on the same plane, thus reducing the overall volume. This structure is easy to realize the omnidirectional radiation characteristics of the antenna, integrate with active devices, and achieve wide-band and direct, inductive coupling and capacitive coupling multiple feed modes [14]. U-shaped ground branches introduced into the antenna floor can be used to increase the bandwidth of the antenna. The antenna radiation patch is slotted and loaded with split ring resonator design to improve impedance matching, increase bandwidth and improve antenna radiation performance.



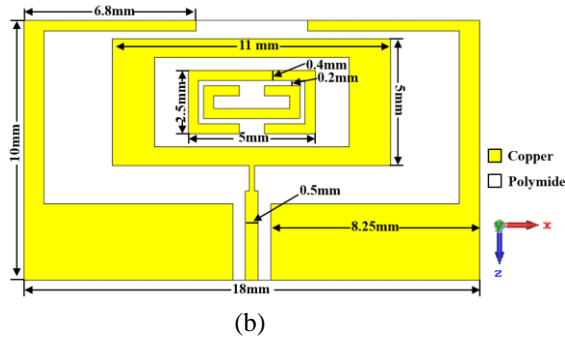


Fig. 1. Schematic diagram of the capsule antenna structure: (a) after conformal and (b) before conformal.

### B. Simulation and measurement environment

This paper used the microwave studio in the CST simulation software to design and simulate the antenna. The modeling and simulation of the antenna adopts the time-domain finite integration method. The numerical calculation process uses Finite Integration Technology (FIT). This numerical solution provides a spatial discrete format to solve a variety of electromagnetic problems. FIT technology spatially visually divides the solving domain, and establishes the integral form of discrete Maxwell equations on each unit surface to realize spatial discretization. In the process of meshing, it is necessary to reach 20-35 mesh lines per wavelength, and it is worth noting that the smallest meshing unit contains at most two mediums.

Since the resonant frequencies of the implanted antennas differ little between the single-layer structure and the multi-layer structure models [15-16], we chose the single-layer structure for calculation and analysis in order to simplify the simulation. The simulation environment is shown in Fig. 2 (a). The size of the model is 100 mm×100 mm×50 mm, and the implantation depth is 10 mm. Based on the antenna design and simulation optimization, the actual processing and production were carried out. The actual antenna and the test scene are shown in Fig. 2 (b). In the 300 MHz ~ 3 GHz frequency band, the dielectric properties of pork and chicken breast are very similar to those of the human body. According to literature research, some design teams conduct tests in pork [17-18], and some teams conduct tests in chicken breast [19-20]. In order to verify the correctness of the simulation results, the antenna was tested in pork and chicken breasts. Two kinds of experimental materials were used to verify the performance of the antenna at the same time, which could strengthen the reliability of the experiment and the practicability of the antenna. The test instrument used the E5063A vector network analyzer produced by Keysight. During the test, a flexible 50 Ω coaxial cable was used to connect the feed port of the antenna and the vector network analyzer (VNA) for measurement.

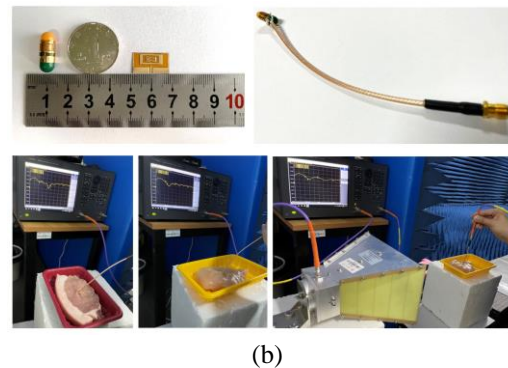
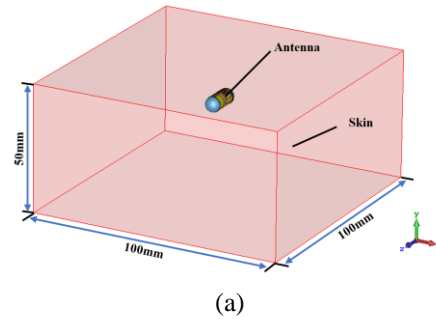


Fig. 2. (a) Schematic diagram of the capsule antenna implanted into the skin model, and (b) implantable conformal antenna structure, and actual test environment setting.

## III. ANTENNA DESIGN AND ANALYSIS

### A. Antenna design process

The dielectric properties of human tissues are different to some extent, so it is difficult for narrowband antennas to overcome the detuning phenomenon in biological tissue environment. In order to ensure the normal operation of the antenna in the wireless capsule speculum system, the capsule antenna achieved broadband characteristics by adding structure or optimizing its structure. The antenna design process is shown in Fig. 3.

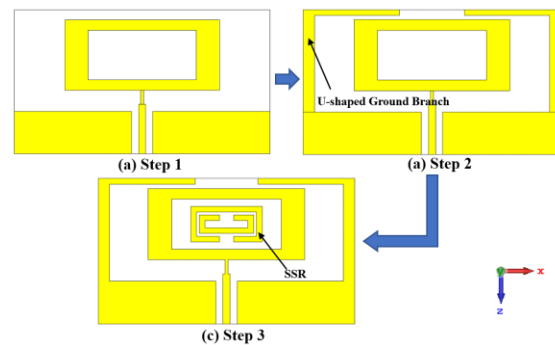


Fig. 3. Implantable antenna design process: (a) unloaded U-shaped ground branch (UGB), (b) unloaded split ring structure (SRR), and (c) final designed antenna structure.

Introduce U-shaped ground branch (UGB): In this design, UGB was introduced on the GND of the antenna to increase the resonance point of the antenna and improve the impedance bandwidth of the antenna. Increasing the U-shaped ground connection in the antenna outer layer is conducive to enlarging the capacitive coupling area between the antenna ground connection and the surrounding frequency band, thereby increasing the electric field strength of the radiating surface [21].

Loaded split ring resonator (SRR): SRR is a metamaterial structural unit with negative permeability properties [22]. When the SRR structure is much smaller than the free wavelength, its structure can be equivalent to an LC resonant circuit. SRR reduces the inductance of the loop, thereby improving the impedance matching characteristics of the antenna [23]. The antenna-loaded SRR structure can not only improve the impedance matching of the antenna and the return loss of the antenna, but also increase the gain of the antenna.

**B. Antenna performance comparison**

The structure of the antenna is optimized through design steps to achieve the desired performance. S11 represents the return loss characteristics of the antenna. Through the combination of the above design methods, the UWB operation of the antenna is realized. Since the dielectric properties of human tissues are complex and changeable, a wider bandwidth helps to resist the drift of resonance frequency, and thus overcome the detuning effect. As shown in Fig. 4, the working frequency band of the antenna is 1.15 GHz - 4.18 GHz, and the absolute bandwidth is 3.03 GHz, covering WMTS frequency band and ISM frequency band, achieving the effect of ultra-wideband. Comparing steps 1, 2 and 3, we can draw the following conclusion. On the basis of coplanar waveguide feeding technology and radiating patch slotting, the antenna improves impedance matching and realizes ultra-wideband characteristics by introducing a combination of UGB and SRR technologies.

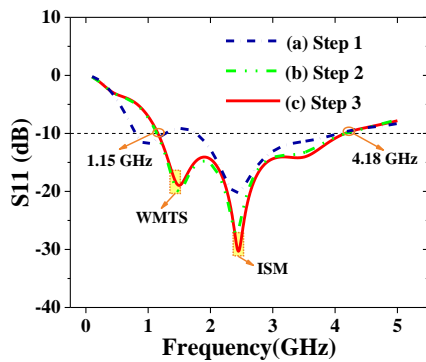


Fig. 5. Comparison of S11 for the steps achieving final design.

As shown in Fig. 5, we expanded the area of the capacitive coupling area of the antenna by loading the SRR and UGB structure, thereby increasing the maximum electric field strength of the original antenna. As the electric field strength of the antenna radiation surface increases, the radiation gain of the antenna will also increase.

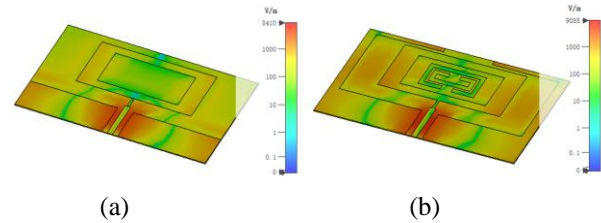


Fig. 5. Electric field of antenna ( $f=2.45$  GHz): (a) without UGB and SRR and (b) with UGB and SRR.

The gain of the implanted antenna is mainly affected by its physical size and working environment. While the implanted antenna is miniaturized, the gain is very low. As shown in Figure 6, the gain of the implanted antenna loaded with UGB or SRR has been improved to a certain extent, mainly in the high frequency region of the working frequency band. Adding SRR and UGB structure to optimize antenna gain. We can see that the two structures are loaded at the same time in the working frequency band of the antenna, which further improves the gain of the antenna.

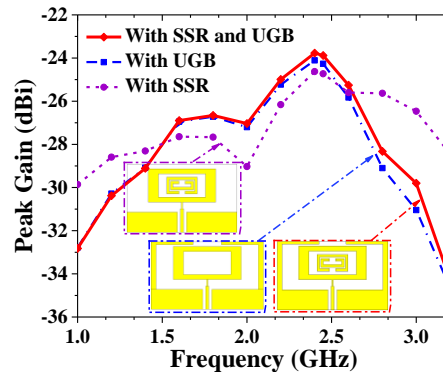


Fig. 6. Antenna gain comparison adding U shaped ground and SRR.

**IV. RESULTS AND DISCUSSION**

The antenna was processed and tested. As shown in Fig. 7, the simulated and measured S11 results are basically consistent. Although the required operating frequency had been shifted in different biological tissues, the two required operating frequency bands were covered quite well. In addition, we observed that the test frequency band was wider than the analog frequency band. In addition to the experimental error caused by the

processing technology, these differences may be attributed to the two factors. First of all, measurements of environmental effects and differences in the dielectric properties of pork and chicken breasts can cause errors. Secondly, the coaxial cable is welded (See in Fig. 2 (b)), which has a certain influence on impedance matching. Due to the limitations of the manufacturing process, these factors are unavoidable. In general, the measurement results verify the correctness of the simulation results.

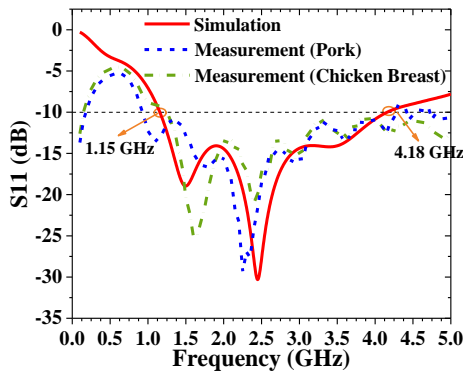


Fig. 7. S11 of the implanted antenna in the simulated and measured environment (pork and chicken breast).

The gain of the antenna represents the ability of the WCE to send and receive signals. For capsule implanted antennas, the gain is generally relatively low. Figure 8 shows the far-field pattern of the antenna at 1.4 GHz and 2.45 GHz. The measurement of the antenna gain was carried out by comparing with the standard gain horn. The designed antenna was tested in pork and chicken breast separately. The maximum gain of the test antenna in the 1 GHz - 3.2 GHz frequency band is shown in Fig. 9. The maximum gain at 1.4 GHz is -29.2 dBi, and the maximum gain at 2.45 GHz is -23.9 dBi. Due to factors such as air loss, feed loss, and test error, the gain of the antenna changes slightly. The actual measured gain is basically consistent with the simulated gain.

Figure 10 shows the antenna radiation efficiency change over frequency band. The antenna works in an implanted environment, and there is a large part of the coupling with the biological environment, and its radiation efficiency is greatly reduced. Generally, the radiation efficiency of implantable antennas is less than 1% [24]. The highest radiation efficiency of the antenna in the target frequency band basically reaches  $8 \times 10^{-4}$ , which is similar to the situation of most implanted antennas. The deviation between simulation and

measurement is mainly caused by environmental interference during the test, but the results are basically consistent.

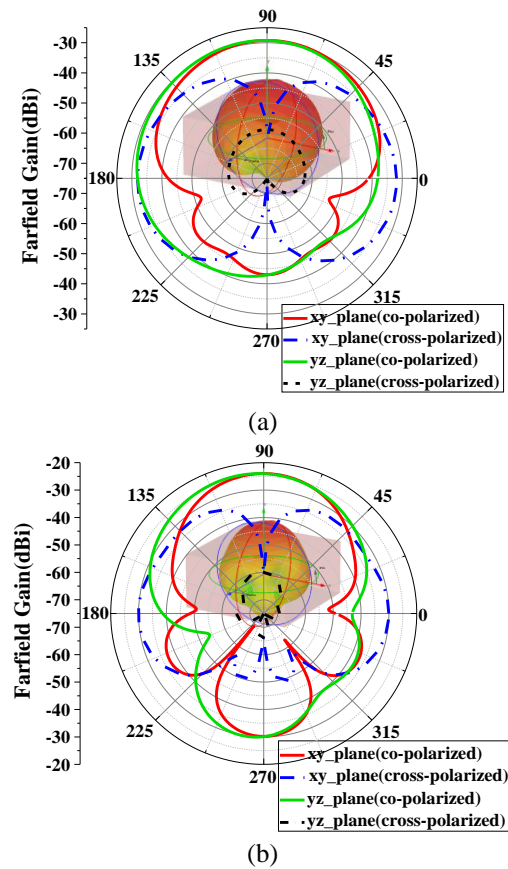


Fig. 8. Gain of the proposed capsule antenna, (a) 1.4 GHz and (b) 2.45 GHz.

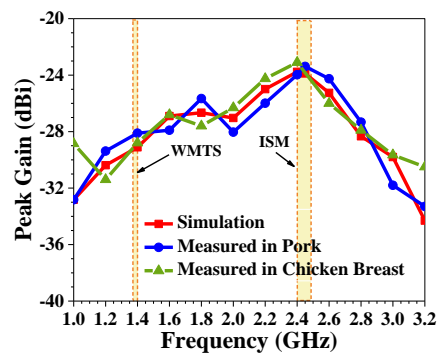


Fig. 9. Gain comparison of the implanted antenna in the simulated and measured environments (pork and chicken breast).



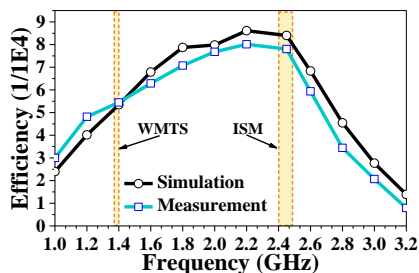


Fig. 10. Simulated and measured radiation efficiency of the proposed antenna.

The working environment of the implanted antenna is special, and we need to ensure the health of the human body. The IEEE C 95.1-1999 standard limits the average specific absorption rate (SAR) of 1g of human tissue to less than 1.6 W/kg, and the average specific absorption rate (SAR) of 10 g human tissues to not exceed 2 W/kg

[25]. When the incident power is set to 1W, the SAR values obtained are 1 g and 10 g, as shown in Table 1, far greater than the specified standard. Therefore, the SAR value is reduced by reducing the incident power to meet the specified criteria. The table also shows the recommended maximum power input as a reference. From the values in the table, we can conclude that the maximum safe input power for 1 g -SAR is 3.3 mW, however, for 10 g -SAR, the maximum allowable input power should be 28 mW. In short, the SAR value calculated in the table complies with IEEE regulations.

As shown in Table 2, the implanted capsule antenna designed in this paper is compared with the antennas in the same type of literatures. Considering multiple parameters of the antenna, we can see that the size of the antenna in this paper is relatively smaller and has a wider bandwidth. This design realized the miniaturization and ultra-wideband of the antenna, while maintaining a better gain.

Table 1: Peak spatial average SAR (input power = 1 W) and maximum allowable input power

Frequency (GHz)	MAX SAR(W/kg)		1g Allowable Input Power (mW)	10g Allowable Input Power (mW)
	1g - Avg	10g - Avg		
1.4	503	82.2	3.2	25
2.45	517	83.1	3.3	28

Table 2: Comparison of the proposed antenna to the same type of capsule antenna literatures

Ref.	Size (mm×mm×mm)	Coverage Frequency Band	10 dB Bandwidth (MHz)	Peak Gain (dBi)	Max-Efficiency (1/1E4)	MAX-SAR(W/kg)	
						1-g	10-g
[7]	16.5×15.7×1.27	MedRadio	162	-37	< 2	485	N.M.
[8]	15×15×0.79	MedRadio	541	-31.5	N.M.	913	N.M.
[9]	28×14×0.254	MICS, ISM	1850	-31.5	N.M.	N.M.	N.M.
[11]	18×18×1.235	MedRadio, ISM	3193	-18.4	2.5-41	216	N.M.
[12]	20×12.6×0.1	ISM	630	-30.6	N.M.	N.M.	N.M.
This study	18×10×0.1	WMTS, ISM	3030	-23.9	8	517	83.1

\*Ref.= Reference. N.M.= not mentioned.

### V. CONCLUSION

In this paper, an ultra-wideband conformal implantable antenna for a wireless capsule endoscope system was designed, which covered WMTS and ISM frequency bands. The structure of the antenna was simulated, analyzed, and optimized, and the ultra-wideband operation was finally realized. The antenna volume was only 18 mm<sup>3</sup>. The antenna adopted the form of UGB and loaded SRR structure to further improve the performance and achieve better radiation. The maximum gain of the antenna was -23.9 dBi. The SAR value of the antenna also meets IEEE regulations. Compared with the ultra-wideband capsule antenna in the previous literatures, it has higher gain, smaller volume and superior performance. The actual measurement results

are in good agreement with the simulation. This paper verified the performance of the antenna through design, analysis and experiments, and provided reference for further research on the application of the conformal capsule antenna.

### REFERENCES

- [1] B. Biswas, A. Karmakar, and V. Chandra, "Miniaturised wideband ingestible antenna for wireless capsule endoscopy," *IET Microwaves, Antennas & Propagation*, vol. 14, no. 4, pp. 293-301, Feb. 2019.
- [2] M. Wang, L. Cai, H. Zheng, and Z. Yang, "Review of flexible antenna technology for electronic capsule," *Electronic Components and Materials*, vol. 36, no. 4, pp. 9-14, Apr. 2017.

- [3] S. Yun, K. Kim, and S. Nam, "Outer-wall loop antenna for ultrawideband capsule endoscope system," *IEEE Antennas and Wireless Propagation Letters*, vol. 9, pp. 1135-1138, Nov. 2010.
- [4] P. M. Izdebski, H. Rajagopalan, and Y. Rahmat-Samii, "Conformal ingestible capsule antenna: A novel chandelier meandered design," *IEEE Transactions on Antennas and Propagation*, vol. 57, no. 4, pp. 900-909, Apr. 2009.
- [5] C. Schmidt, F. Casado, A. Arriola, I. Ortego, P. D. Bradley, and D. Valderas, "Broadband UHF implanted 3-D conformal antenna design and characterization for in-off body wireless links," *IEEE Transactions on Antennas and Propagation*, vol. 62, no. 3, pp. 1433-1444, Mar. 2014.
- [6] B. Huang, G. Yan, P. Zan, and Q. Li, "Design of the microstrip antenna for radiotelemetry capsule," *Journal of Shanghai Jiaotong University*, vol. 41, no. 11, pp. 1830-1833, Nov. 2007.
- [7] L. J. Xu, Y. X. Guo, and W. Wu, "Bandwidth enhancement of an implantable antenna," *IEEE Antennas and Wireless Propagation Letters*, vol. 14, pp. 1510-1513, Nov. 2014.
- [8] J. Wang, M. Leach, E. G. Lim, Z. Wang, R. Pei, and Y. Huang, "An implantable and conformal antenna for wireless capsule endoscopy," *IEEE Antennas and Wireless Propagation Letters*, vol. 17, no. 7, pp. 1153-1157, May 2018.
- [9] S. Kim and H. Shin, "An ultra-wideband conformal meandered loop antenna for wireless capsule endoscopy," *Journal of Electromagnetic Engineering and Science*, vol. 19, no. 2, pp. 101-106, Dec. 2019.
- [10] X. Cheng, D. Senior, C. Kim, and Y. K. Yoon, "A compact omnidirectional self-packaged patch antenna with complementary split-ring resonator loading for wireless endoscope applications," *IEEE Antennas Wireless Propag. Lett.*, vol. 10, pp. 1532-1535, Dec. 2011.
- [11] Z. Jiang, Z. Wang, M. Leach, E. G. Lim, J. Wang, R. Pei, and Y. Huang, "Wideband loop antenna with split-ring resonators for wireless medical telemetry," *IEEE Antennas and Wireless Propagation Letters*, vol. 18, no. 7, pp. 1415-1419, July 2019.
- [12] B. Biswas, A. Karmakar, and V. Chandra, "Fractal inspired miniaturized wideband ingestible antenna for wireless capsule endoscopy," *AEU-International Journal of Electronics and Communications*, vol. 120, pp. 153192, June 2020.
- [13] Z. Duan, Y. X. Guo, M. Je, and D. L. Kwong, "Design and in vitro test of a differentially fed dual-band implantable antenna operating at MICS and ISM bands," *IEEE Trans. Antennas Propag.*, vol. 62, no. 5, pp. 2430-2439, Feb. 2014.
- [14] W. Liu and X. Yang, "Design of electrically small slot antenna fed by CPW," *Chinese Journal of Electron Devices*, vol. 42, no. 2, pp. 300-303, Apr. 2019.
- [15] J. Kim and Y. Rahmat-Samii, "Implanted antennas inside a human body: Simulations, designs, and characterizations," *IEEE Transactions on Microwave Theory and Techniques*, vol. 52, no. 8, pp. 1934-1943, Aug. 2004.
- [16] T. Karacolak, A. Z. Hood, and E. Topsakal, "Design of a dual-band implantable antenna and development of skin mimicking gels for continuous glucose monitoring," *IEEE Transactions on Microwave Theory and Techniques*, vol. 56, no. 4, pp. 1001-1008, Apr. 2008.
- [17] J. Shang and Y. Yu, "An Ultrawideband capsule antenna for biomedical applications," *IEEE Antennas Wireless Propag. Lett.*, vol. 18, no. 12, pp. 2548-2551, Dec. 2019.
- [18] V. Kaim, B. K. Kanaujia, S. Kumar, H. C. Choi, K. W. Kim, and K. Rambabu, "Ultra-miniature circularly polarized CPW-fed implantable antenna design and its validation for biotelemetry applications," *Scientific Reports*, vol. 10, no. 1, pp. 1-16, Apr. 2020.
- [19] S. Das and D. Mitra A, "compact wideband flexible implantable slot antenna design with enhanced gain," *IEEE Transactions on Antennas and Propagation*, vol. 66, no. 8, pp. 4309-4314, May 2018.
- [20] W. Cui, R. Liu, L. Wang, M. Wang, H. Zheng, and E. Li, "Design of wideband implantable antenna for wireless capsule endoscope system," *IEEE Antennas and Wireless Propagation Letters*, vol. 18, no. 12, pp. 2706-2710, Dec. 2019.
- [21] C. Y. Huang, C. L. Tsai, and C. L. Yang, "Compact broadband implantable monopole antenna with gain enhancement," *2014 IEEE Antennas and Propagation Society International Symposium (APSURSI)*. IEEE, pp. 1590-1591, July 2014.
- [22] R. A. Shelby, D. R. Smith, S. C. Nemat-Nasser, and S. Schultz, "Microwave transmission through a two-dimensional, isotropic, left-handed metamaterial," *Appl. Phys. Lett.*, vol. 78, no. 4, pp. 489-491, Jan. 2001.
- [23] R. S. Alrawashdeh, Y. Huang, M. Kod, and A. A. B. Sajak, "A broadband flexible implantable loop antenna with complementary split ring resonators," *IEEE Antennas and Wireless Propagation Letters*, vol. 14, pp. 1506-1509, Feb. 2015.
- [24] M. Zada and H. Yoo, "Miniaturized dual band antennas for intra-oral tongue drive system in the ISM bands 433 MHz and 915 MHz: Design, safety, and link budget considerations," *IEEE Transactions on Antennas and Propagation*, vol. 67, no. 9, pp. 5843-5853, Sept. 2019.
- [25] IEEE Standard for Safety Levels with Respect to Human Exposure to Radio Frequency Electromagnetic Fields, 3 kHz to 300 GHz, *IEEE Standard C95.1-1999*, 1999.